

## X-ray yields in protonium and mesic hydrogen

E. Borie

*Institut für Theoretische Kernphysik der Universität Karlsruhe, 7500 Karlsruhe, West Germany*

M. Leon

*Los Alamos Scientific Laboratory, Los Alamos, New Mexico 87545*

(Received 24 October 1979)

Recent experimental investigations of atomic x rays in protonium have revived interest in the atomic cascade process. Following a calculation of Leon and Bethe, which includes chemical and Auger deexcitation, Stark mixing and annihilation, as well as radiative transitions, we investigate the dependence of the yields of  $K$  and  $L$  x rays on the target density, and on the hadronic shifts and widths of the  $1s$  and  $2p$  levels. Numerical results are also given for kaonic, pionic, and muonic hydrogen.

### I. INTRODUCTION

Recent investigations of atomic x rays in various forms of exotic hydrogen have revived interest in the subject of the atomic cascade process. The relevant processes—Stark mixing, absorption due to the strong interaction, chemical and Auger deexcitation, as well as radiative transitions, were investigated some time ago by Leon and Bethe<sup>1</sup> (hereafter referred to as LB). In particular, as was first pointed out by Day, Snow, and Sucher,<sup>2</sup> the Stark mixing was shown to induce substantial absorption of pions and kaons from high- $n$  states, resulting in a substantial reduction of both the x-ray yields and the cascade time. Similar investigations were carried out for antiprotons by Desai<sup>3</sup> and by Dalkarov *et al.*<sup>4</sup> However, these authors neglected the  $l$  dependence of the Auger and radiative transition rates. The purpose of the present work is to adapt the calculation of Leon and Bethe<sup>1</sup> to the study of exotic hydrogen as a function of target density, and to investigate the sensitivity of the cascade process to such things as Stark mixing rates, kinetic energy of the atom, hadronic shifts, and widths, etc. It is hoped that such information will be of assistance in the planning of experiments.

Although the calculation is based on that of LB, some changes have been made. The calculation of the various processes which affect the cascade will be summarized in Sec. II. Section III will deal with our results for the cases of muonic, pionic, kaonic, and antiprotonic hydrogen. A comparison with the available experimental data will be made.

### II. PROCESSES WHICH AFFECT THE CASCADE

After capture in an initial state with  $n \approx \sqrt{M_K}$  ( $M_K$  is the reduced mass of the system, in units of the electron mass), deexcitation proceeds mainly

by Auger ionization of the neighboring hydrogen atoms, or by “chemical” dissociation of the hydrogen molecules. (Using a distribution of  $n > \sqrt{M_K}$  as the starting value would result in an increase of the cascade time by up to 30%, but has little effect on the yields, absorption probabilities, etc.) As in LB, we take the rates to be given approximately by

$$\begin{aligned} \Gamma_{if}(\text{chem}) &\approx \frac{1}{2} N v \pi a_{n_i}^2 \quad \text{if } \Delta E > 4.7 \text{ eV} \\ \Gamma_{if}(\text{Aug}) &\approx \frac{16}{3} \pi \frac{N}{M_K^2} R_{if}^2 (2\Delta E + 1.39)^{-1/2} \\ &\quad \text{if } \Delta E > 15.2 \text{ eV} \approx 0.56 \text{ Ry.} \end{aligned} \quad (1)$$

Here  $R_{if}$  is the radial matrix element for the transition  $n_i l_i$  to  $n_f l_f$  with  $l_f = l_i \pm 1$ ,  $N$  is the density of hydrogen atoms,  $v$  is the velocity of the exotic atom, and  $a_{n_i}$  is the radius of its  $n_i$ th Bohr orbit.

The rates for radiative deexcitation are given, as usual, by

$$\Gamma_{if}(\text{rad}) = \frac{4}{3} \alpha \hbar^{-1} M_K^{-2} R_{if}^2 (\Delta E)^3. \quad (2)$$

The relative importance of the radiative and Auger rates depends on the target density and on the type of atom. For the case of pions (or muons) stopping in liquid hydrogen, radiation is unimportant for transitions such that  $n_f > 3$ . The relative importance of radiative transitions increases as the target density is decreased (the radiative and Auger rates for pionic hydrogen are comparable for  $n = 6$  at a gas pressure of 1 atm). The corresponding  $n$  values are larger if the negatively charged particle is heavier.

#### A. Absorption

The rates for hadronic absorption are given by

$$\Gamma_{ns} \approx \Gamma_{1s}/n^3, \quad \Gamma_{np} \approx \frac{32}{3} \frac{(n^2 - 1)}{n^5} \Gamma_{2p}. \quad (3)$$

The widths  $\Gamma_{1s}$  and  $\Gamma_{2p}$ , as well as the shift  $\delta E_{1s}$ , are input parameters. They can be related to the imaginary part of the complex scattering length by

$$\begin{aligned}\Gamma_{1s}/2 &= 2\pi |\psi_{1s}(0)|^2 M_K^{-1} \text{Im}(A_s) \\ &= (1.56 \times 10^{12} \text{ fm}^{-1} \text{ s}^{-1}) M_K^2 \text{Im}(A_s),\end{aligned}\quad (4a)$$

$$\begin{aligned}\Gamma_{2p}/2 &= 6\pi |\nabla\psi_{2p}(0)|^2 M_K^{-1} \text{Im}(A_p/k^2) \\ &= (52.3 \text{ fm}^{-3} \text{ s}^{-1}) M_K^4 \text{Im}(A_p/k^2),\end{aligned}\quad (4b)$$

provided the scattering-length approximation for calculating the level width of a hadronic atom is valid.

### B. Stark mixing

Transitions among the  $n^2$  degenerate states of a given  $n$  are induced when the hadronic atom passes near, or through, a hydrogen atom and "feels" the electric field due to the hydrogen atom. (Coulomb deexcitation is also possible, as has been discussed by Fiorentini.<sup>5</sup> However, Stark mixing is probably more important.) Although this work is based on LB, we treat the Stark mixing somewhat differently here. In order to better describe the  $n$  region where Auger and/or radiation become competitive with Stark mixing (as happens in a gas), we use a shuffling model. This presents a difficulty compared with the usual cascade model in that probability is transferred back and forth among the  $l$  states at each value of  $n$ . We circumvent this by using a difference equation for the *arrival probability*. This is solved using standard methods for the inversion of banded matrices. The shuffle rates are calculated using the relation

$$\Gamma_{n l - n l - 1} = \frac{2l + 1}{2l - 1} \Gamma_{n l - n l + 1} = \pi N v \rho_0^2 \quad (5)$$

for  $l > 1$  where, as in LB,  $\rho_0$  is an effective impact parameter. It is the root of the equation

$$\frac{v M_K}{2n^2} = \frac{\xi(\rho)}{\rho} = \frac{1}{\pi\rho} \int_{-\pi/2}^{\pi/2} e^{-2\rho \sec\theta} (1 + 2\rho \sec\theta + 2\rho^2 \sec^2\theta) d\theta. \quad (6)$$

If an  $s$  state is involved, the removal of the degeneracy of the energy levels by the strong interaction (and, where appropriate, by vacuum polarization) hinders the Stark mixing, since the electric field must overcome the energy difference between the  $ns$  and  $np$  states. This is taken into account by using a different (and smaller) impact parameter  $R_0$ . According to LB, the fraction  $R(\gamma)$  of atoms which mixes with the  $ns$  state can be approximated by

$$R(\gamma) = 1 \text{ if } |\gamma| = \frac{|5E_{ns}|}{3n^2 F(R)} M_K < 0.58 \quad (R < R_0), \quad (7)$$

where  $F(R) = (1 + R^{-1} + R^{-2}/2) \exp(-2R)$ . It follows

that  $R_0$  is the root of

$$F(R) = (0.5747/n^5) M_K |\delta E_{1s}|. \quad (8)$$

For small values of  $n$  ( $< 8$ ), it is more appropriate to take  $R_0$  as the impact parameter for which

$$\frac{\Gamma_{ns}}{nv} \int_{-\infty}^{\infty} \frac{dX}{3|\gamma^2(R)|} = 1,$$

or

$$\int_{-\infty}^{\infty} dX F^2(R) = \frac{M_K^2 v}{3n^5 \Gamma_{1s}} |\delta E_{1s}|^2. \quad (9)$$

In practice  $R_0$  is computed by both methods, and the larger of the two is taken. We then have

$$\Gamma_{np - ns} = \frac{1}{3} \Gamma_{ns - np} = \pi N v R_0^2. \quad (10)$$

The shift  $\delta E_{1s}$  in Eqs. (8) and (9) was taken as an effective shift, such that

$$|\delta E_{1s}|_{\text{eff}} = |\delta E_{1s}(\text{had}) + \delta E_{1s}(\text{vp}) - i\Gamma_{1s}/2|.$$

We assume that the energy shift of the  $np$  state is negligible.

## III. NUMERICAL RESULTS

### A. Antiprotons

For the case of the  $p\bar{p}$  system, the interesting observable quantities are the hadronic shift and width of the  $1s$  and  $2p$  states, including spin dependence, and the probability for annihilation from a  $p$  state. Experimentally, Bailey *et al.*<sup>6</sup> have set a lower limit on  $\Gamma_{2p}$  (probably spin averaged):

$$\Gamma_{2p} > 10\Gamma_{2p}(\text{rad}) = 0.004 \text{ eV}.$$

An estimate by Kaufmann and Pilkuhn,<sup>7</sup> based on a black-disc model, predicts  $\Gamma_{2p} \approx 100\Gamma_{2p}(\text{rad}) \approx 0.04$  eV (spin averaged). We have considered both of these possibilities in the calculations.

At the present time little is known about the shift and width of the  $1s$  state. From the scattering lengths of Bryan and Phillips,<sup>8</sup> one obtains

$$\delta E_{1s} - i\Gamma_{1s}/2 = \begin{cases} (610-750i) \\ (950-625i) \\ (870-650i) \end{cases}$$

in eV, for the singlet, triplet, and spin-averaged cases, respectively. We also considered the possibility  $-\delta E_{1s} \approx \Gamma_{1s} \approx 1000$  eV.

Since experimental information on the yield of  $L$  x rays in a gas target at 4 atm and ambient temperature is available, a systematic study of the sensitivity of the yields of  $K$  and  $L$  x rays at this target density, as a function of the velocity of the  $p\bar{p}$  atom, Stark mixing coefficient  $k_{\text{STK}}$  (an arbitrary factor multiplying all Stark mixing rates), and annihilation width of the  $2p$  state was under-

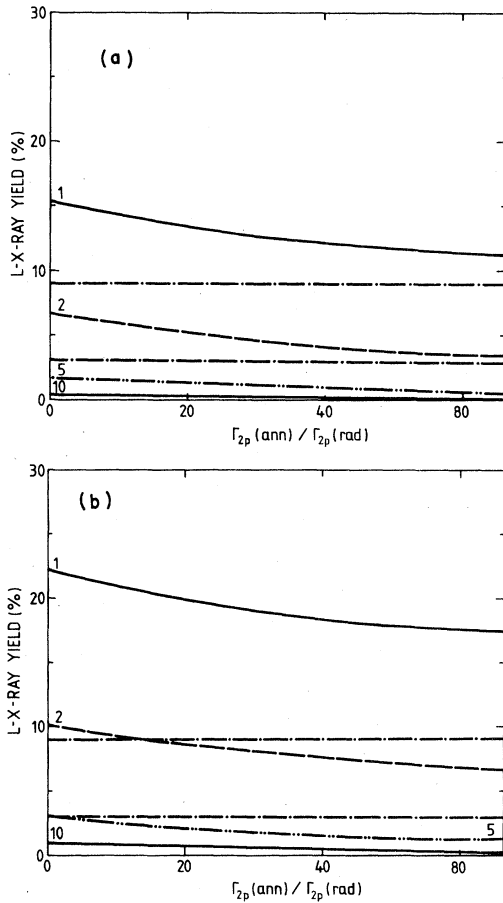


FIG. 1.  $L$ -x-ray yields as a function of the ratio  $\Gamma_{2p}(\text{ann})/\Gamma_{2p}(\text{rad})$  for antiprotons stopped in gaseous hydrogen at 4-atm pressure and room temperature.  $\Gamma_{1s} = -\delta E_{1s} \approx 1$  keV. The numbers labeling the curves give the Stark coefficient. Dot-dashed lines: experimental limits for yield ( $Y_{\text{expt}} = 6 \pm 3\%$ ). (a)  $T = 1$  eV, (b)  $T = \frac{1}{4}$  eV.

taken. For this exercise, the hadronic width and shift of the  $1s$  state were held fixed at 1 keV. The results are shown in Figs. 1 ( $L$  yield) and 2 ( $K$  yield). The x ray yields are plotted as a function of  $\Gamma_{2p}/\Gamma_{2p}(\text{rad})$  for various values of  $T_{\text{atom}}$  ( $T_{\text{atom}} = 1$  eV corresponds to  $v = 10^6$  cm) and Stark coefficient. The Stark mixing rates are proportional to the product  $v \cdot k_{\text{STK}}$ , since the impact parameter depends only very weakly on the velocity. A comparison of the curves in Figs. 1(a) and 1(b), or 2(a) and 2(b) reveals that the yields depend on these parameters individually, and not simply on their product. The yields are also very sensitive to the value of the Stark coefficient. For the velocities under consideration, a value of Stark coefficient between 2 and 5 gives a reasonable fit to the data (horizontal dashed-dotted lines in Fig. 1). The decrease in yield as the Stark mixing rates

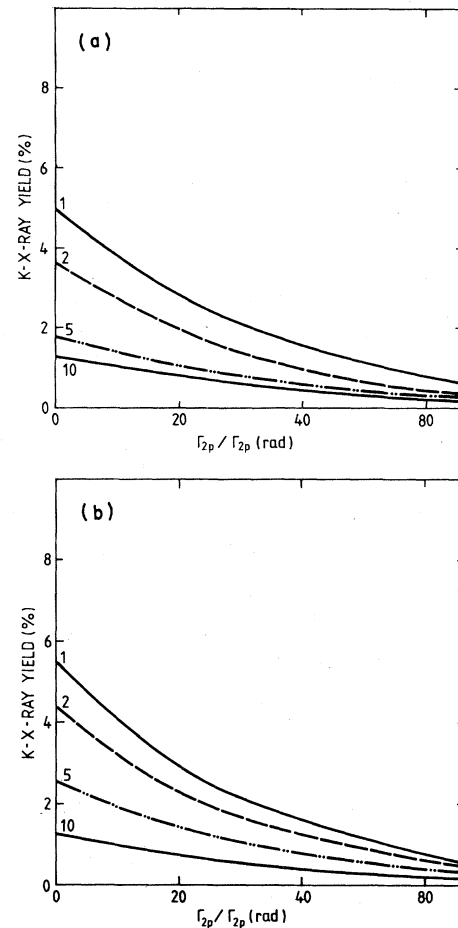


FIG. 2.  $K$ -x-ray yields as a function of the ratio  $\Gamma_{2p}(\text{ann})/\Gamma_{2p}(\text{rad})$  for a gas target. Description of curves as in Fig. 1.

are increased is easy to understand. As the probability for mixing with a high- $n$   $s$  state is increased, the probability that the system annihilates from a high  $s$  state is increased. In addition, there is considerable  $p$ -state annihilation from states with  $n = 6, 7, 8$ ; this is also affected by the Stark mixing. The available data can be fitted with values of  $\Gamma_{2p}$  between 4 and 40 meV; however, smaller Stark mixing rates are required as  $\Gamma_{2p}$  is increased.

Figures 3, 4, and 5 show the total  $L$  x-ray yield, the total  $K$  x-ray yield, and the probability for absorption from a  $p$  state as a function of target density. Figures 3(a), 4(a), and 5(a) show the results obtained with  $\Gamma_{2p} = 4$  meV,  $|\delta E_{1s}| = \Gamma_{1s} = 1$  keV for several values of  $k_{\text{STK}}$  and  $T_{\text{atom}}$  which gave reasonable fits to the data at 4 atm. The dashed curves are similar, except that  $\Gamma_{2p} = 40$  meV. The curves in Figs. 3(b), 4(b), and 5(b) were calculated using the predictions for  $\Gamma_{1s}$  and  $\delta E_{1s}$  from the

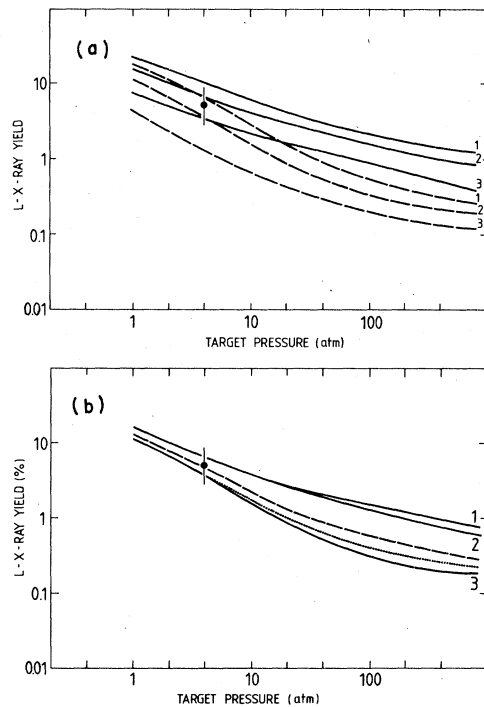


FIG. 3.  $L$ -x-ray yield for protonium as a function of target pressure. Experimental points from Ref. 6. (a)  $\Gamma_{1s} \approx -\delta E_{1s} = 1$  keV. Solid curves:  $\Gamma_{2p}(\text{ann})/\Gamma_{2p}(\text{rad}) = 10$ ; dashed curves:  $\Gamma_{2p}(\text{ann})/\Gamma_{2p}(\text{rad}) = 100$ . Curves 1:  $k_{\text{STK}} = 2$ ,  $T = \frac{1}{4}$  eV; curves 2:  $k_{\text{STK}} = 2$ ,  $T = 1$  eV; curves 3:  $k_{\text{STK}} = 5$ ,  $T = \frac{1}{4}$  eV. (b)  $k_{\text{STK}} = 2$ ,  $T = 1$  eV.  $\Gamma_{1s}$  and  $\delta E_{1s}$  from the Bryan-Phillips model. See text for further description.

scattering lengths of Bryan and Phillips. The curves labeled 1 were calculated using the spin-averaged  $1s$  shift and width, and  $\Gamma_{2p} = 4$  meV. Curves labeled 2 were calculated using the spin-singlet parameters for the  $1s$  state and  $\Gamma_{2p} = 4$  meV. The curves labeled 3 were calculated using the spin-triplet scattering lengths for the shift and width of the  $1s$  state, and  $\Gamma_{2p} = 40$  meV; they differ insignificantly from those calculated using the spin-averaged shift and width for the  $1s$  state and  $\Gamma_{2p} = 40$  meV. The results shown in curves 2 and 3 were spin averaged to give the dashed curves. It makes a difference whether the spin averaging for the  $2p$  state is done before or after the cascade calculation. Since the cascade is too fast to allow any significant singlet-triplet transitions, the latter is more appropriate. The dotted curves give results obtained with  $\Gamma_{2p} = 31$  meV. The extreme sensitivity of all yields to  $\Gamma_{2p}$  should be noticed.

Our predictions for the probability of annihilation from a  $p$  state in liquid range from 5 to 45%, depending on the values of  $\Gamma_{2p}$  and the Stark mixing

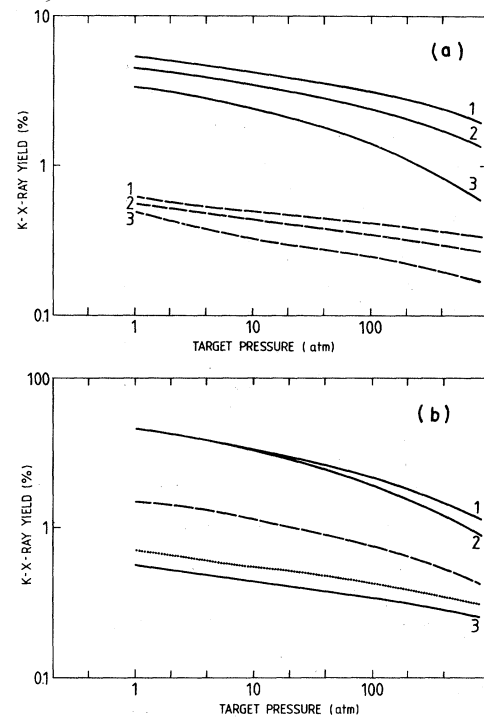


FIG. 4. Same as Fig. 3, for yield of  $K$  x rays as function of target density.

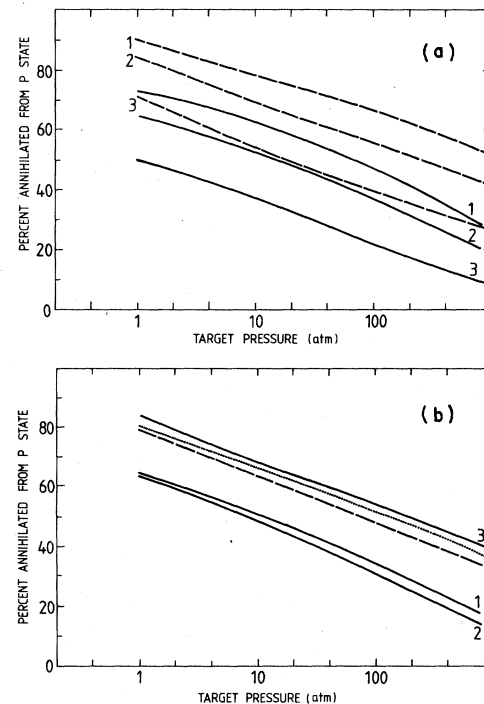


FIG. 5. Probability of  $\bar{p}p$  annihilation from a  $p$  state as a function of target density. Explanation of curves as for Fig. 3.

coefficient, as can be seen in Figs. 5(a)–5(c). With a smaller Stark mixing coefficient, and/or smaller width of the  $1s$  state, even larger values have been obtained. As was first pointed out in Ref. 2, Stark mixing increases the probability for annihilation from  $s$  states with high principal quantum number  $n$ , and thus reduces the total absorption from  $p$  states (as well as the x-ray yields), so this result is not surprising. The experimental situation regarding  $\bar{p}p$  annihilation from  $p$  states is unclear. Evidence from the process

$$\bar{p}p \rightarrow \pi^0 \pi^0$$

indicates a substantial probability for  $p$ -state annihilation,<sup>9</sup> which in turn would favor a larger value of  $\Gamma_{2p}$  and smaller Stark mixing ( $k_{\text{STK}} < 5$ ). On the other hand, experiments on the process

$$\bar{p}p \rightarrow K_0 \bar{K}_0$$

indicate a significantly smaller  $p$ -state annihilation probability,<sup>10,11</sup> which would favor  $\Gamma_{2p} \approx 10$  meV and a somewhat larger Stark mixing coefficient

( $k_{\text{STK}} > 3$ ). It is also possible<sup>12</sup> that the annihilation to  $\pi^0 \pi^0$  takes place in two steps:

$$\begin{aligned} \bar{p}p \Big|_{\text{atomic state}} &\rightarrow \bar{p}p \Big|_{\text{tightly bound nuclear state}} + \gamma \\ \bar{p}p \Big|_{\text{tightly bound nuclear state}} &\rightarrow \pi^0 \pi^0 \end{aligned}$$

If this is the case, what appears to be  $p$ -wave annihilation is really  $s$ -wave absorption. One could obtain a useful constraint on the parameters of this calculation if the probability for annihilation from a  $p$  state as a function of the target density were better known experimentally.

Figures 6 show the relative  $K$  yields  $K\alpha/(\text{all } K)$ ;  $K\beta/(\text{all } K)$ , etc. as a function of the unshifted x-ray energy for  $\bar{p}$  stopped in liquid hydrogen. These quantities are mainly sensitive to the width of the  $2p$  state, and rather insensitive to Stark mixing and to the shift and width of the  $1s$  state. In general, an increase in the Stark mixing rates enhances the transitions ( $n > 5 \rightarrow n = 1$ ). Figure 6(a) uses values for the shift and width of the  $1s$  state suggested by Izycki *et al.*<sup>13</sup> ( $\Gamma_{1s} = 250$  eV,  $\delta E_{1s} = -2500$  eV). Figure 6(b) corresponds to  $\Gamma_{1s} = \delta E_{1s} = 1$  keV. In all cases the  $K\alpha$  and  $K\beta$  lines are very weak and most of the x-ray intensity is concentrated in the 4–1 and 5–1 (or 5–1 and 6–1) transitions. It is therefore unlikely that the pattern sought by Izycki *et al.*<sup>13</sup> could have been seen.

The total  $K$ -x-ray intensity is more sensitive to the Stark mixing, velocity, and shift and width of the  $1s$  level, as can be seen from Figs. 4(a)–4(c). The branching ratios also become more sensitive to these quantities in a gas target, as can be seen in Fig. 7, where the ratio of  $K\alpha$  to all  $K$  is plotted as a function of target density for two different

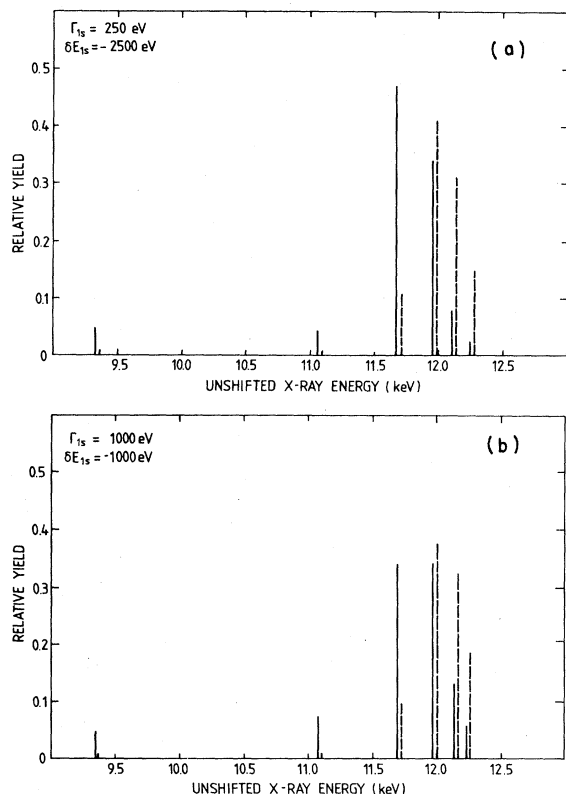


FIG. 6. Relative  $K$ -x-ray yields (normalized to total yield 1) as a function of unshifted x-ray energy (in keV). Solid lines:  $\Gamma_{2p} = 4$  meV; dashed lines:  $\Gamma_{2p} = 40$  meV. In (a), we take  $\Gamma_{1s} = 250$  eV,  $\delta E_{1s} = -2500$  eV; (b) corresponds to  $\Gamma_{1s} = -\delta E_{1s} = 1000$  eV.  $k_{\text{STK}} \sqrt{T} \approx 2$  for both figures.

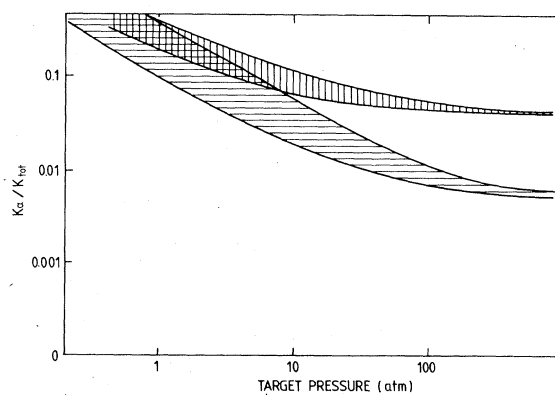


FIG. 7. Relative yield  $K\alpha/K_{\text{tot}}$  for  $K$  x rays as a function of target pressure.  $1s = 1-1.5$  keV,  $\delta E_{1s} = -1$  to  $-2$  keV.  $k_{\text{STK}} \sqrt{T}$  varies from 1 to 2.5. Vertical bars: range of values for  $\Gamma_{2p} = 4$  meV. Horizontal bars: range of values for  $\Gamma_{2p} = 40$  meV.

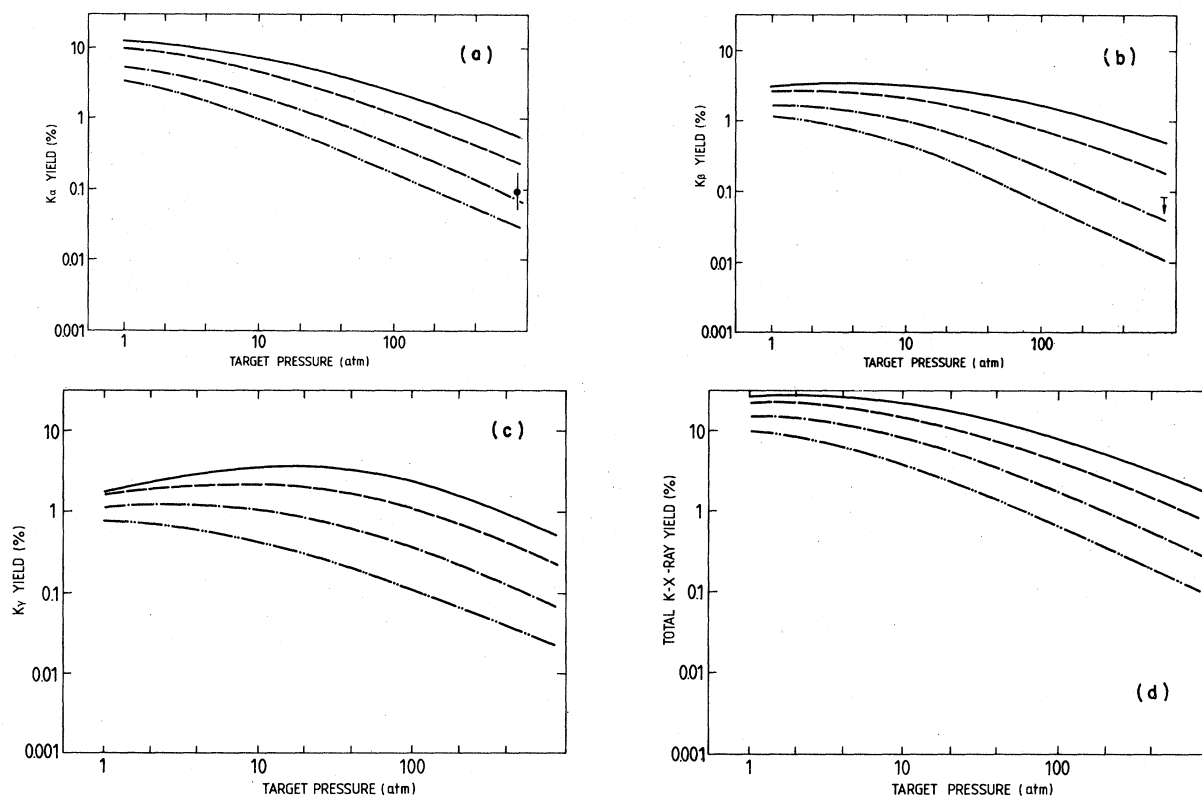


FIG. 8.  $K$ -x-ray yield for  $K^*p$  as a function of target pressure (ambient temperature).  $\Gamma_{2p}(\text{ann})=10^{-4}$  eV;  $\Gamma_{1s}=250$  eV,  $\delta E_{1s}=125$  eV; Solid curve:  $k_{\text{STK}}=2$ ,  $T=\frac{1}{4}$  eV; dashed curve:  $k_{\text{STK}}=2$ ,  $T=1$  eV; — · —:  $k_{\text{STK}}=5$ ,  $T=\frac{1}{4}$  eV; — · · —:  $k_{\text{STK}}=5$ ,  $T=1$  eV. (a)  $K\alpha$  yield; (b)  $K\beta$  yield; (c)  $K\gamma$  yield; (d)  $K_{\text{tot}}$  yield. Experimental points in (a) and (b) from Ref. 14.

values of  $\Gamma_{2p}$ . The bands indicate the maximum variation which was obtained for Stark coefficient between 2 and 5 for several values of velocity.

#### B. Kaons

A recent experiment from the Rutherford Laboratory<sup>14</sup> has reported observing the  $K\alpha$  x ray from kaonic hydrogen with an intensity of  $(0.11 \pm 0.06)\%$  per stopped kaon. The hadronic shift and width were reported to be  $40 \pm 60$  eV and  $<250$  eV, respectively. The shift of the  $K\alpha$  line due to vacuum polarization is about 25 eV. The  $K\beta$  line was not observed, and an upper limit on its intensity of about half that of the  $K\alpha$  line was reported.

The observed shift and width of the  $1s$  state are not in accordance with what one would expect from the scattering-length approximation. However, the presence of a subthreshold resonance—the  $Y^*(1405)$  in the  $K^*p$  system makes it unlikely that the scattering-length approximation is valid in this case. The results of our calculations for the observed shift and width of the  $1s$  state and for  $\Gamma_{2p}=10^{-4}$  eV [note that  $\Gamma_{2p}(\text{rad})=2.6 \times 10^{-4}$  eV] are shown in Figs. 8, 9, and 10. Here we plotted the

$K\alpha$ ,  $K\beta$ , and  $K\gamma$  yields, as well as the total  $K$  yields, cascade time, and percent absorbed from a  $p$  state, as a function of density for several combinations of Stark coefficient and atomic kinetic energy. The results on the  $K\alpha$  yield are not

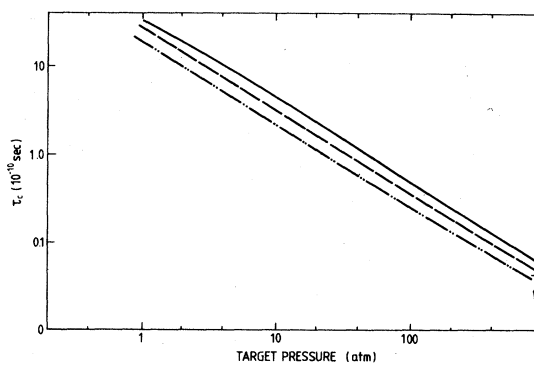


FIG. 9. Cascade time (in units of  $10^{-10}$  s) for kaonic hydrogen as function of the target pressure. Parameters and notation for curves as for Figs. 8(a)–8(d). (The dashed curve is identical to the dash-dot curve.) Experimental limit from Ref. 15.

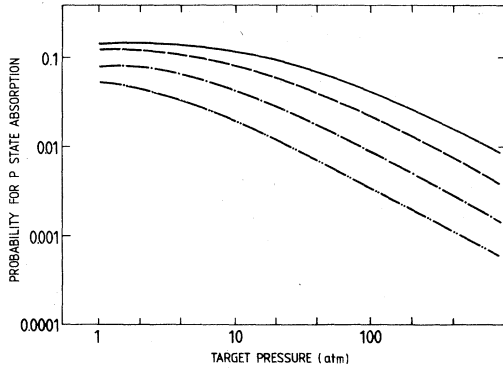


FIG. 10. Percent of kaons absorbed from  $p$  state as function of the target density. Parameters and notation as for Fig. 8.

inconsistent with the experiment of Davies *et al.*<sup>14</sup> for Stark mixing coefficient 2–5 ( $k_{\text{STK}} = 1$  results in too large a yield). It is not possible to fit the observed branching ratio  $K\beta/K\alpha < \frac{1}{2}$  (in liquid) with a larger value of  $\Gamma_{2p}$ . The predicted yields are also too low if  $\Gamma_{2p}(\text{abs}) > \Gamma_{2p}(\text{rad})$ . The calculated cascade time is somewhat too high [(5–6)  $\times 10^{-12}$  s as compared to an experimental upper limit<sup>15</sup> of  $4 \times 10^{-12}$  s]. The cascade time can be reduced by about 20%, with no significant change in the calculated yields, by reducing the initial value of  $n$  (from 25 to 23) or by doubling the rates for chemical deexcitation. These results are not very sensitive to  $\delta E_{1s}$ . Here we use  $\Gamma_{1s} = 250$  eV, and  $\delta E_{1s} = 125$  eV. The dashed curves and the dash-dot curves would be the same if  $\Gamma_{1s} = \delta E_{1s} = 80$  eV. If we take  $\Gamma_{1s} = 250$  eV, and  $\delta E_{1s} = 80$  eV, the  $K\alpha$  yields in liquid are reduced 10–20%, but are hard-

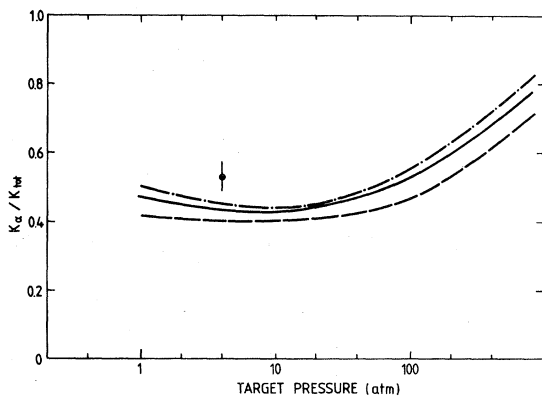


FIG. 11.  $K\alpha/K_{\text{tot}}$  as a function of target pressure for pionic hydrogen.  $\Gamma_{1s} = 0.82$  eV. Data point from Ref. 20. Solid curve:  $k_{\text{STK}} = 2$ ,  $\delta E_{1s} = 5.7$  eV,  $T = \frac{1}{4}$  eV, and  $T = 1$  eV; also  $k_{\text{STK}} = 2$ ,  $\delta E_{1s} = 2$  eV,  $T = 1$  eV. Dashed curve:  $k_{\text{STK}} = 5$ ,  $\delta E_{1s} = 10$  eV,  $T = 1$  eV, and  $\delta E_{1s} = 5.7$  eV,  $T = \frac{1}{4}$  eV. Dash-dot curve:  $k_{\text{STK}} = 1$ ,  $T = 1$  eV,  $\delta E_{1s} = 5.7$  eV.

ly changed at all for a gas target.

For the case of kaons stopped in a dilute gas, the cascade time is comparable to the kaon lifetime, and a significant fraction (>10%) of the kaons decay before they complete the cascade. A substantial fraction is also absorbed from a  $p$  state ( $2p$  to  $6p$ ). The long cascade times for kaons stopping in a dilute gas might permit the detection of the decaying kaons; the time distribution of the decays could also yield useful information.

### C. Pions

For the case of pions, the width of the  $1s$  level has been fairly reliably determined from experiments on charge exchange at low energies and on the radiative capture process.<sup>16</sup> We have used

$$\Gamma_{1s} = 0.82 \text{ eV.}$$

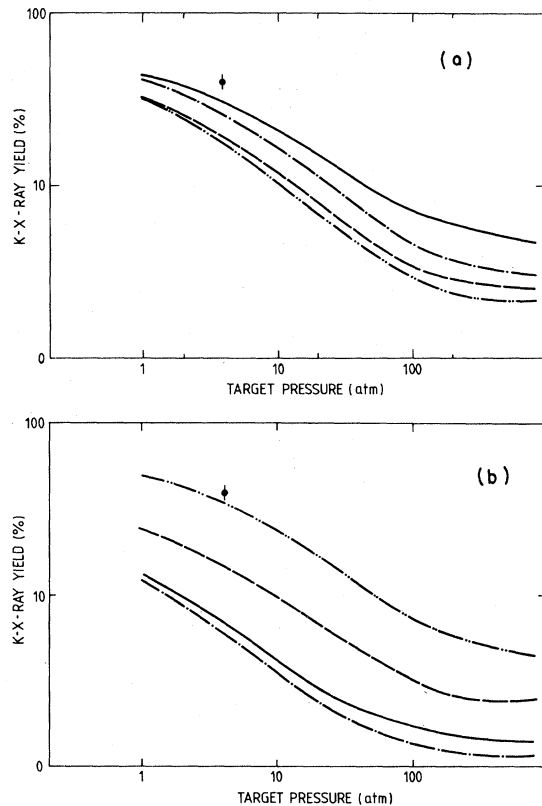


FIG. 12. Total  $K$ -x-ray yield (in %) for pionic hydrogen as a function of target pressure.  $\Gamma_{1s} = 0.82$  eV. Data from Ref. 20. (a)  $k_{\text{STK}} = 2$ . Solid curve:  $T = \frac{1}{4}$  eV,  $\delta E_{1s} = 5.7$  eV; dashed curve:  $T = 1$  eV,  $\delta E_{1s} = 5.7$  eV; dash-dot curve:  $T = \frac{1}{4}$  eV,  $\delta E_{1s} = 2$  eV; dash-dot-dot curve:  $T = 1$  eV,  $\delta E_{1s} = 2$  eV; (b) Solid curve:  $k_{\text{STK}} = 5$ ,  $T = 1$  eV,  $\delta E_{1s} = 10$  eV; dashed curve:  $k_{\text{STK}} = 5$ ,  $T = \frac{1}{4}$  eV,  $\delta E_{1s} = 10$  eV; dash-dot curve:  $k_{\text{STK}} = 5$ ,  $T = 1$  eV,  $\delta E_{1s} = 5.7$  eV; dash-dot-dot curve:  $k_{\text{STK}} = 1$ ,  $T = 1$  eV,  $\delta E_{1s} = 5.7$  eV.

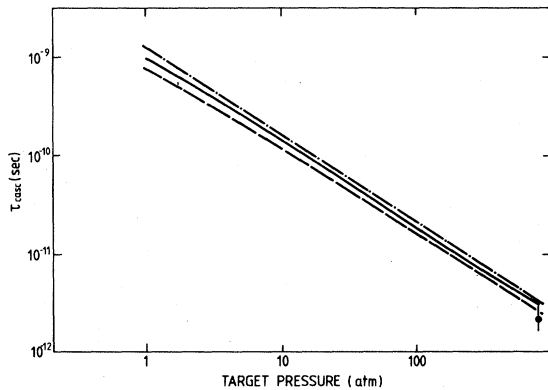


FIG. 13. Cascade times (in units  $10^{-10}$  s) in pionic hydrogen as a function of target pressure.  $\Gamma_{1s} = 0.82$  eV. Data from Ref. 19. Solid curve:  $k_{\text{STK}} = 5$ ,  $T = \frac{1}{4}$  eV,  $\delta E_{1s} = 10$  eV, and  $k_{\text{STK}} = 2$ ,  $T = 1$  eV,  $\delta E_{1s} = 5.7$  eV, 2 eV; dashed curve:  $k_{\text{STK}} = 5$ ,  $T = 1$  eV,  $\delta E_{1s} = 5.7$  eV, 10 eV; dash-dot curve:  $k_{\text{STK}} = 1$ ,  $T = 1$  eV,  $\delta E_{1s} = 5.7$  eV, and  $k_{\text{STK}} = 2$ ,  $T = \frac{1}{4}$  eV,  $\delta E_{1s} = 5.7$  eV, 2 eV.

The real part of the  $\pi^-p$  scattering length has been determined from measurements on pionic atoms,<sup>17</sup> and by dispersion methods<sup>18</sup>. The results are nearly identical, and give

$$\text{Re}a_{\pi^-p} = 0.98 \text{ m}_\pi^{-1},$$

which results in less binding:

$$\delta E_{1s} = -5.7 \text{ eV}.$$

The vacuum polarization shift of the 1s level in pionic hydrogen increases the binding by

$$\delta E_{\text{vp}} = 7.7 \text{ eV}.$$

For pionic hydrogen, absorption from  $p$  states is negligible.

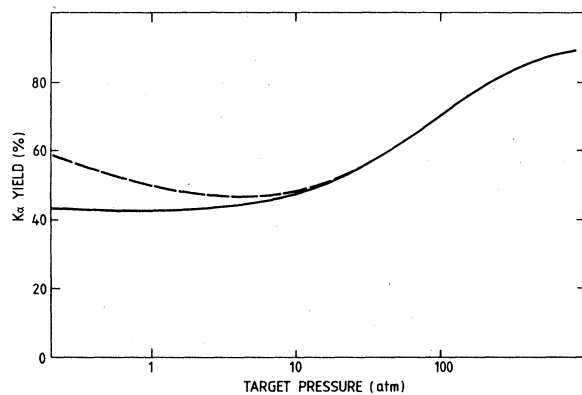


FIG. 14.  $K\alpha$ -x-ray yield in muonic hydrogen as a function of target density. Solid curve:  $k_{\text{STK}} = 10$ ,  $T = 1$  eV. Dashed curve:  $k_{\text{STK}} = 1$ ,  $T = \frac{1}{4}$  eV. Results for intermediate values of these parameters lie between these curves.

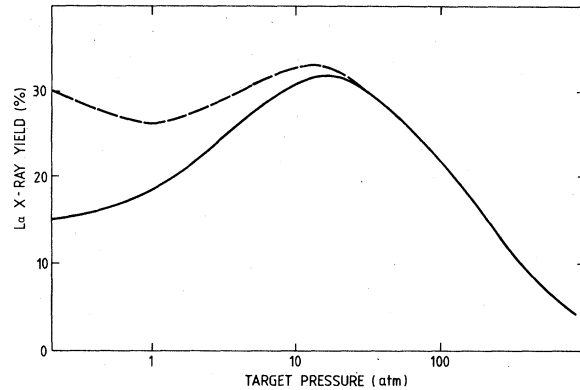


FIG. 15.  $L\alpha$ -x-ray yield in muonic hydrogen as a function of target pressure. Curves denoted as in Fig. 14.

Experimental information<sup>19</sup> exists for the cascade time in a liquid target [ $\tau_c = (2.3 \pm 0.6) \times 10^{-12}$  s], for the total  $K$ -x-ray yield and for the ratio of  $K\alpha$  to all  $K$  in a gas<sup>20</sup> at 4 atm:

$$K\alpha/K_{\text{tot}} = 0.53 \pm 0.04,$$

where  $K_{\text{tot}} = 0.40 \pm 0.04$  per stopped  $\pi^-$ . These quantities, as well as the results of our calculations, are shown in Figs. 11–13. For these, we fixed the value of  $\Gamma_{1s}$  at 0.8 eV and varied  $\delta E_{1s}$ ,  $T_{\text{at}}$ , and the Stark mixing coefficient. Figure 11 shows the ratio of  $K\alpha$  to  $K_{\text{tot}}$  as a function of the target density. Our predictions are uniformly smaller than the experimental value (ranging from 0.40 to 0.45) and are insensitive to all of the parameters which were varied except for the Stark mixing rates.

On the other hand, the total  $K$ -x-ray yield is sensitive to the velocity and to  $\delta E_{1s}$  as well as to the Stark mixing coefficient, as can be seen in Figs. 12. Only a fairly small value of Stark co-

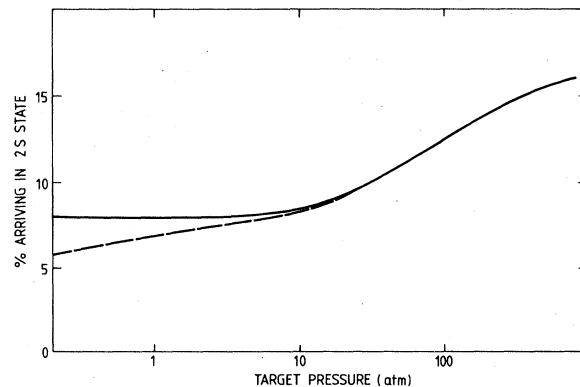


FIG. 16. Percent of muons arriving in the 2s state as a function of target pressure. Curves denoted as in Fig. 14.



efficient ( $k_{\text{STK}} < 2$ ) approaches being consistent with the observed yields. However, our results for the cascade time (Fig. 13) favor larger Stark mixing rates. As for kaons, the cascade times could be reduced by decreasing the initial value of  $n$  or by increasing the rates for chemical de-excitation.

#### D. Muons

Figures 14–16 show our results for muons ( $K\alpha$  and  $L\alpha$  yields, and the percent arriving in the 2s state). These results depend on the kinetic energy of the muonic hydrogen atom, Stark mixing rates, etc., only in a gas target at a pressure below about 5 atm. The two curves shown indicate the maximum variation which was found when the Stark coefficient was varied from 1 to 10 and the atomic kinetic energy from  $\frac{1}{4}$  to 1 eV. (The solid curve gives our results for  $k_{\text{STK}} = 10$ ,  $T_a = 1$  eV, and the dashed curve for  $k_{\text{STK}} = 1$ ,  $T_a = \frac{1}{4}$  eV). The small  $L$ -x-ray yield and the large  $K$ -x-ray yield found in liquid are easily explained by the fact that the Auger rates dominate for  $n$  as low as 3 at liquid density. Our predictions for the  $K\alpha$  yield at pressures below 1 atm are in reasonable agreement with the reported experimental results.<sup>21, 22</sup>

#### IV. SUMMARY

With reasonable values of arbitrarily adjustable parameters, it is possible to fit the available experimental data on x-ray yields in exotic hydrogen fairly well. More data would be required to determine these parameters with any degree of reliability, however. Contrary to popular belief, Stark mixing remains an important factor in the cascade process even in a gas at target pressures as low as 1 atm. In the case of antiprotons and kaons, direct absorption from  $p$  states plays an important role (this effect is negligible for pions and muons). Because of Stark mixing, the yields are insensitive to the initial distribution of stopping mesons (or antiprotons). The cascade times are somewhat sensitive to the initial  $n$  distribution, however.

#### ACKNOWLEDGMENTS

One of the authors (E. B.) wishes to thank the Theory Division at Los Alamos Scientific Laboratory for its kind hospitality during the initial phases of this work. This work was supported in part by the Bundesministerium für Forschung und Technologie and in part by the U. S. Department of Energy.

<sup>1</sup>M. Leon and H. A. Bethe, Phys. Rev. **127**, 636 (1962).

<sup>2</sup>T. B. Day, G. A. Snow, and J. Sucher, Phys. Rev. Lett. **3**, 61 (1959).

<sup>3</sup>B. R. Desai, Phys. Rev. **119**, 1385 (1960).

<sup>4</sup>O. D. Dalkarov, B. O. Kerbikov, and V. E. Markushin, Yad. Fiz. **25**, 853 (1977) [Sov. J. Nucl. Phys. **25**, 455 (1977)].

<sup>5</sup>L. Bracci and G. Fiorentini, Nuovo Cimento A **43**, 9 (1978).

<sup>6</sup>E. G. Auld *et al.*, Phys. Lett. **77B**, 454 (1978).

<sup>7</sup>W. B. Kaufmann and H. Pilkuhn, Phys. Rev. C **17**, 215 (1978).

<sup>8</sup>R. A. Bryan and R. J. N. Phillips, Nucl. Phys. **B5**, 201 (1968).

<sup>9</sup>S. Devons *et al.*, Phys. Rev. Lett. **27**, 1614 (1971).

<sup>10</sup>R. Armenteros *et al.*, *Proceedings of the 1962 International Conference on High Energy Physics at CERN*, edited by J. Prentki (CERN, Geneva, 1962).

<sup>11</sup>C. Baltay *et al.*, Phys. Rev. Lett. **15**, 532 (1965).

<sup>12</sup>P. Pavlopoulos *et al.*, Phys. Lett. **72B**, 415 (1978).

<sup>13</sup>M. Izycki *et al.*, Contribution to the 4th European Antiproton Symposium, Barr, France, 1978 (unpublished).

<sup>14</sup>J. D. Davies *et al.*, Phys. Lett. **83B**, 55 (1979).

<sup>15</sup>R. Knop *et al.*, Phys. Rev. Lett. **14**, 767 (1965).

<sup>16</sup>H. W. Baer, K. Crowe, and P. Truol, *Advances in Nuclear Physics* (Plenum, New York, 1977), Vol. 9, Chap. 3.

<sup>17</sup>L. Tauscher and W. Schneider, Z. Phys. **271**, 409 (1974).

<sup>18</sup>G. Höhler, F. Kaiser, R. Koch, and E. Pietarinen, Handbook of Pion Nucleon Scattering, ZAED Physics Data 12-1, 1979 (unpublished).

<sup>19</sup>J. H. Doede *et al.*, Phys. Rev. **129**, 2808 (1963).

<sup>20</sup>J. Bailey *et al.*, Phys. Lett. **33B**, 369 (1970).

<sup>21</sup>A. Anderhub *et al.*, Phys. Lett. **71B**, 443 (1977).

<sup>22</sup>P. O. Egan *et al.*, Contribution to the Eighth International Conference on High Energy Physics and Nuclear Structure, Vancouver, 1979 (unpublished).